(PbS)32: A baby crystal

B. Kiran, Anil K. Kandalam, Rameshu Rallabandi, Pratik Koirala, Xiang Li et al.

Citation: J. Chem. Phys. **136**, 024317 (2012); doi: 10.1063/1.3672166
View online: http://dx.doi.org/10.1063/1.3672166
View Table of Contents: http://jcp.aip.org/resource/1/JCPSA6/v136/i2
Published by the American Institute of Physics.

$(PbS)_{32}$: A baby crystal

B. Kiran,[1,a)] Anil K. Kandalam,[2] Rameshu Rallabandi,[1] Pratik Koirala,[2] Xiang Li,[3] Xin Tang,[3] Yi Wang,[3] Howard Fairbrother,[3] Gerd Gantefoer,[4] and Kit Bowen[3,a)]
[1]*Department of Chemistry, McNeese State University, Lake Charles, Louisiana 70609, USA*
[2]*Department of Physics, McNeese State University, Lake Charles, Louisiana 70609, USA*
[3]*Departments of Chemistry and Material Sciences, Johns Hopkins University, Baltimore, Maryland 21218, USA*
[4]*Department of Physics, University of Konstanz, 78457 Konstanz, Germany*

(Received 4 November 2011; accepted 5 December 2011; published online 11 January 2012)

Theoretical calculations based on density functional theory have found $(PbS)_{32}$ to be the smallest cubic cluster for which its inner $(PbS)_4$ core enjoys bulk-like coordination. Cubic $(PbS)_{32}$ is thus a "baby crystal," i.e., the smallest cluster, exhibiting sixfold coordination, that can be replicated to obtain the bulk crystal. The calculated dimensions of the $(PbS)_{32}$ cluster further provide a rubric for understanding the pattern of aggregation when $(PbS)_{32}$ clusters are deposited on a suitable surface, i.e., the formation of square and rectangular, crystalline nano-blocks with predictable dimensions. Experiments in which mass-selected $(PbS)_{32}$ clusters were soft-landed onto a highly ordered pyrolytic graphite surface and the resulting aggregates imaged by scanning tunneling microscopy provide evidence in direct support of the computational results. © *2012 American Institute of Physics*. [doi:10.1063/1.3672166]

INTRODUCTION

Ultra-small aggregates of lead sulfide have attracted considerable attention in recent years due to their unusual properties.[1–4] While most studies have focused on colloidal nanoparticles of lead sulfide,[5] work on isolated (gas phase) clusters of lead sulfide, $(PbS)_n$, has been relatively scarce. Recently, in a combined experimental and theoretical study[6] we explored the geometric structures and electron affinities of gas-phase lead sulfide clusters, $(PbS)_n$, ranging in size from $n = 1$–15. With its large highest occupied molecular orbital (HOMO)- lowest unoccupied molecular orbital (LUMO) gap and as the preferred product of cluster fragmentation, $(PbS)_4$ was shown to be the most stable of the lead sulfide clusters studied. This result is also consistent with the fact that the primitive cell in crystalline lead sulfide is made up of four lead sulfide molecules. In addition, we found a growth pattern, over this size range, which gave rise to two-dimensional arrangements of lead sulfide cuboids, i.e., each additional PbS molecule adding to the existing cluster in a planar (side by side) rather than a three-dimensional fashion. This restricted the maximum coordination number for lead and sulfur atoms to five, rather than the sixfold coordination found in bulk, lead sulfide crystals.

Since the foregoing sizes of lead sulfide clusters are too small to adopt bulk-like sixfold coordination, what is the smallest $(PbS)_n$ cluster size that can do so *and* that can also be replicated to form the bulk material? In this contribution, we demonstrate that $n = 32$ is this critical size, i.e., $(PbS)_{32}$ is a cubic "baby crystal." We further show that the successive fusion of multiple $(PbS)_{32}$ units is well on its way toward forming the bulk crystalline structure of lead sulfide. We also present experimental results that support our computational findings.

a)Authors to whom correspondence should be addressed. Electronic addresses: kiran@mcneese.edu and kbowen@jhu.edu.

COMPUTATIONAL METHODS AND RESULTS

We have utilized two types of computational methods in the current study. For small cluster sizes ($n = 4$–32), the calculations were carried out using the GAUSSIAN 03 program.[7] The PW91PW91 density functional,[8,9] along with the SBKJC[10] basis set for lead and the 6–311G* basis for sulfur atoms, were used for these calculations. The accuracy of this method has been established in our previous study.[6] For larger, composite clusters that contain multiple $(PbS)_{32}$ units, Gaussian-based calculations are prohibitively expensive, and thus for these, we have used the DMOL3 program suite.[11] For these clusters, the PW91 functional,[12] along with the Double Numerical plus d-functions (DND) and Density functional Semi-core PseudoPotentials (DSPP) basis sets,[13] were used. All the clusters were optimized with the appropriate symmetry constraints.

Since $(PbS)_4$ is the cluster size that mimics the primitive cell of crystalline lead sulfide, the smallest cluster that has sixfold coordination and can also be replicated to form bulk crystalline lead sulfide, viz., the "baby crystal," will be composed of an integer number of $(PbS)_4$ units. We hypothesize that the successive *dimerization* of $(PbS)_{4n}$ cluster units, i.e., $4n = 4 \rightarrow 8 \rightarrow 16 \rightarrow 32 \ldots$ will eventually lead us to this baby crystal. The dimerization of a given cluster can occur in two ways: (1) dimerization in a plane (length-wise), leading to a two-dimensional arrangement and (2) dimerization out of plane (height-wise), leading to a three-dimensional stacking of cuboids. We have considered a number of $(PbS)_{4n}$ clusters. The optimized structures of these $(PbS)_{4n}$ clusters are presented in Figures 1 and 2.

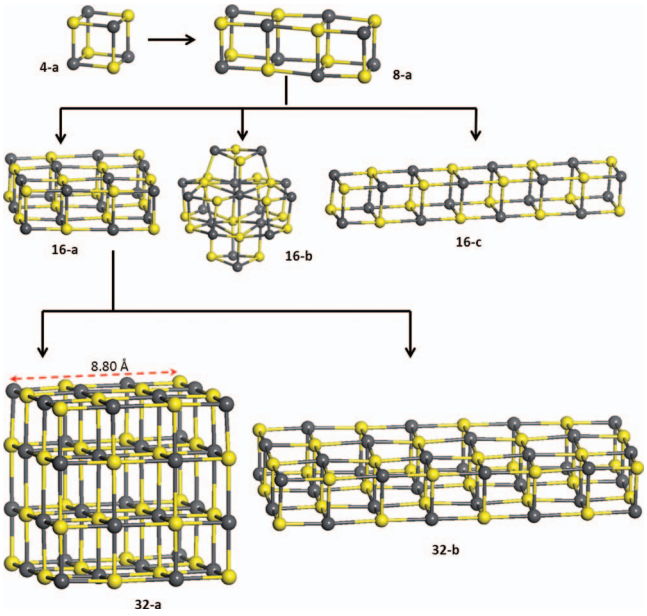

FIG. 1. The growth pattern of lead sulfide cluster structures via dimerization of $(PbS)_{4n}$ units. For $(PbS)_{16}$ and $(PbS)_{32}$, both, the lowest, (a), and higher, ((b) and (c)), energy isomers are shown.

As noted in our earlier work,[6] $(PbS)_4$ forms a cube and $(PbS)_8$ forms a di-cube due to the dimerization of two $(PbS)_4$ cuboids (see structures, **4-a** and **8-a**, respectively in Figure 1). We have also calculated a number of geometries for $(PbS)_{16}$. There, the lowest energy isomer is the one where two $(PbS)_8$ units have dimerized to form a square structure (**16-a**) (fusion in a plane). While the three-dimensional structure, **16-b**, contains several atoms with sixfold coordination, this isomer is 0.84 eV higher in energy than structure, **16-a**. Furthermore, the quadrangular prism, **16-c**, which is an end-on-end, dimeric extension of structure, **8-a** is 1.15 eV higher in energy than structure, **16-a**. The dimerization of **16-a** can proceed either by horizontal or vertical stacking, leading to two isomers, **32-a** and **32-b**. The most stable isomer, **32-a**, is a large three-dimensional cube (T_d symmetry) with an edge length of 8.8 Å; it is the result of the vertical stacking of $(PbS)_{16}$ units. The 4×8 rectangular structure, **32-b**, which resulted from horizontal dimerization of $(PbS)_{16}$ units, is 1.90 eV higher in energy. Several other geometrical isomers, which include both two- and three-dimensional arrangements of cuboidal units, were also considered and found to be higher in energy than the T_d structure (**32-a**). Structure **32-a** is the first in this series of clusters, which were formed by the dimerization of $(PbS)_{4n}$ units, to attain sixfold coordination. With this attribute and an inner geometric structure that is qualitatively identical to that of the bulk crystal, structure **32-a** is certainly a candidate for being the "baby crystal."

Having explored the dimerization of $(PbS)_{4n}$ clusters and having established that $(PbS)_{32}$ exhibits sixfold coordination and forms a 3D structure which mimics that of the bulk, we ask the question: are there even smaller clusters which both exhibit sixfold coordination and possess the same structure as the bulk? In other words, is $(PbS)_{32}$ the smallest such cluster; is it *the* baby crystal? In order to answer this question, we have computed the structures of $(PbS)_{4n}$ clusters, where $n = 5$, 6, and 7. Structures of these clusters are shown in Figure 2. The most stable geometry of $(PbS)_{20}$ is the 4×5 rectangular structure, **20-a**. Its three-dimensional isomer, **20-b**, is 0.23 eV higher in energy. Isomer **20-a** is a rectangular derivative of the $(PbS)_{16}$ cluster structure, **16-a** and does not contain any atoms with sixfold coordination. The most stable isomers of $(PbS)_{24}$ and $(PbS)_{28}$ are structures, **24-a** and **28-a**, respectively. The 4×6 rectangular structure of $(PbS)_{24}$, **24-b**, is 0.86 eV higher in energy than structure **24-a**, while the 4×7 rectangular structure of $(PbS)_{28}$, **28-b**, is 0.93 eV higher in energy than structure **28-a**. Structures, **24-a** and **28-a** both contain atoms exhibiting sixfold coordination. Thus, one can conclude that the onset of sixfold coordination in $(PbS)_{4n}$ clusters occurs at cluster size, $4n = 24$, i.e., at $n = 6$. However, neither **24-a** or **28-a** possess the structure of the bulk crystal, and thus neither can be replicated to form the bulk material. Thus, structure **32-a** of $(PbS)_{32}$ is *the* baby crystal. Interestingly, structures, **24-a** and **28-a** can be obtained from structure, **32-a** by removing PbS units, although their structures will distort as a result. This further supports the proposition that the cubic $(PbS)_{32}$ skeleton, structure **32-a**, is structurally very robust.

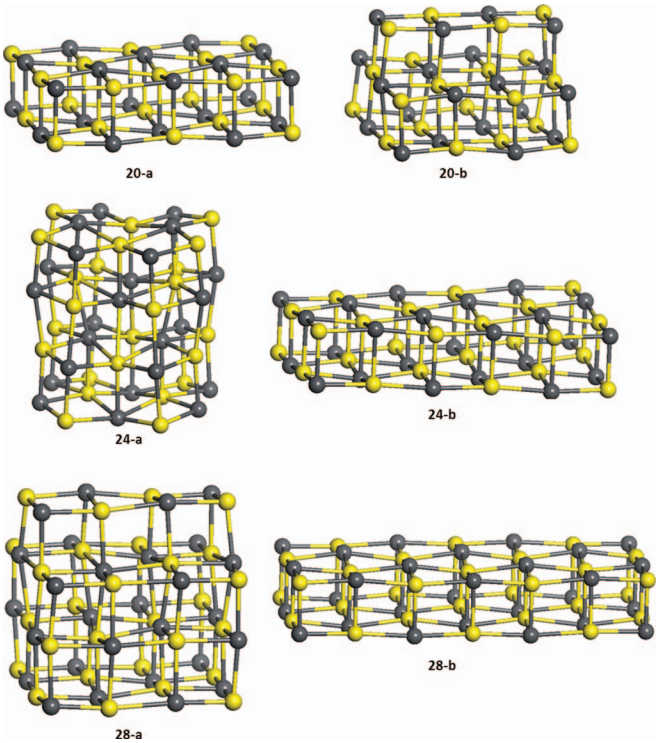

FIG. 2. Structures of lowest, (a), and higher, (b), energy isomers of $(PbS)_{4n}$ ($n = 5$, 6, and 7).

As the nascent (baby) nano-crystal of lead sulfide, $(PbS)_{32}$ should be thermodynamically stable relative to neighboring lead sulfide cluster sizes. In order to gauge the thermodynamic stability of $(PbS)_{32}$, we have used the following expression to calculate the energy required to remove a $(PbS)_4$ unit from each of the $(PbS)_{4n}$ clusters:

$$\text{Energy to remove a } (PbS)_4 \text{ unit} = -[E(PbS)_{4n} - E(PbS)_{4n-4} - E(PbS)_4]. \quad (1)$$

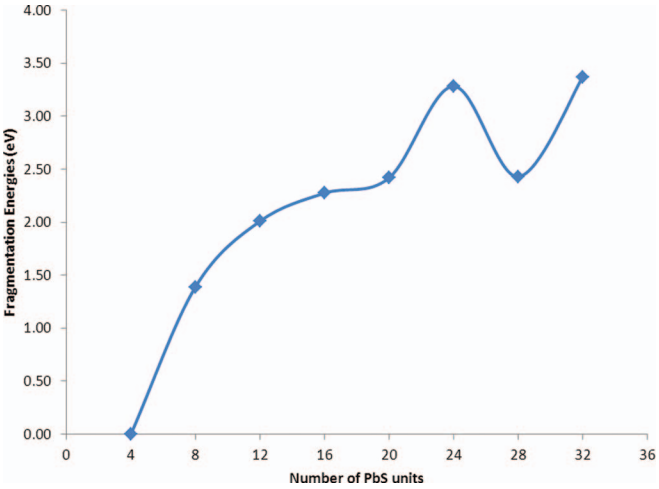

FIG. 3. Fragmentation energy of $(PbS)_{4n}$ clusters ($n = 1$–8) versus the number of PbS molecular units. Fragmentation products are: $(PbS)_{4n-4} + (PbS)_4$.

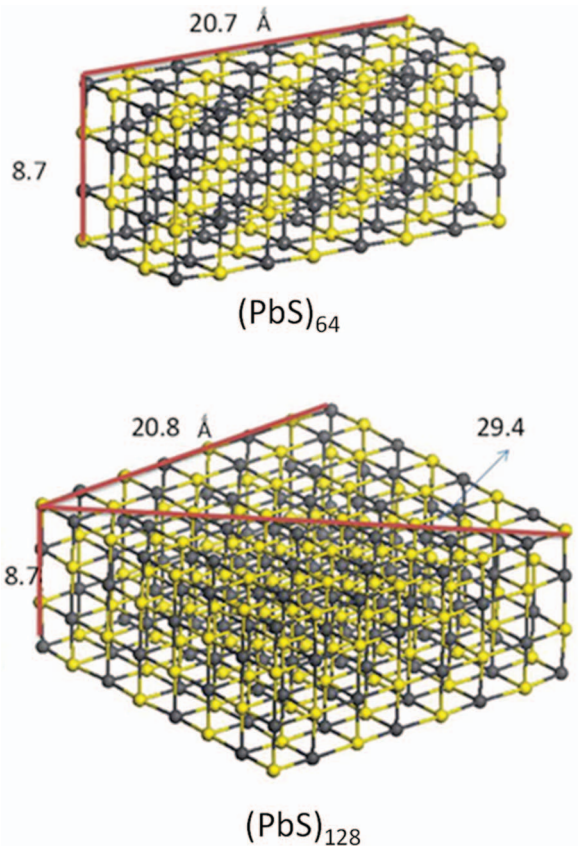

FIG. 4. Calculated lowest energy structures for the $(PbS)_{64}$ and $(PbS)_{128}$ nano-blocks.

In this equation, the energies correspond to the ground state isomers of the parent and the fragmentation products. Figure 3 presents these fragmentation energies as a function of the number of PbS units in a given cluster, $4n$. It is evident from the graph that as the cluster size increases, the energy required to fragment $(PbS)_{4n}$ into $(PbS)_4$ and $(PbS)_{4n-4}$ increases smoothly up to $4n = 20$. At $4n = 24$, there is a sharp increase in the fragmentation energy, reflecting the first structural transformation from two-dimensional to three-dimensional stacking of $(PbS)_4$ cuboids. A second maximum appears at $n = 32$, indicating that cubic $(PbS)_{32}$, i.e., structure **32-a**, is also highly stable against fragmentation. By comparison, the fragmentation energy for structure **32-b**, formed by a two-dimensional $(PbS)_4$ cuboid growth pattern, is 2.23 eV, which is significantly lower than that for isomer **32-a**. As for structure, **24-a**, while it is comparably stable with respect to fragmentation, and while its inner $(PbS)_4$ unit has also attained the required sixfold coordination, structure **24-a** does not possess the same structural framework as the bulk lead sulfide crystal, and thus, continued replication of $(PbS)_{24}$ units can not lead to bulk formation. On the other hand, structure **32-a** of $(PbS)_{32}$ possesses the same structural framework as the bulk lead sulfide crystal, exhibits sixfold coordination, and is highly stable against fragmentation. Therefore, $(PbS)_{32}$ can be considered to be *the* "baby crystal" – the smallest possible stable cluster, which upon replication leads to the bulk structure. Structure **32-a** is the seed of lead sulfide crystal growth.

Additional calculations showed that cubical $(PbS)_{32}$ baby crystals can assemble two-dimensionally to form yet larger clusters made up of multiple $(PbS)_{32}$ units. Our calculations also showed that these composite clusters prefer to form square or rectangular objects, and that these nano-crystals have theoretically predictable dimensions. For example, two $(PbS)_{32}$ units can dimerize to form a rectangular $(PbS)_{64}$ nano-block with dimensions, $2.07 \times 0.88 \times 0.88$ nm, and two $(PbS)_{64}$ units can dimerize to form a square $(PbS)_{128}$ nano-block with dimensions, $(2.08 \times 2.08 \times 0.88)$ nm. Figure 4 shows the resulting calculated nano-crystal structures. Allowing these "nano-blocks" to grow on a surface and then determining their resultant dimensions is the basis of the complementary experiments described below.

EXPERIMENTAL METHODS AND RESULTS: SUPPORTING EVIDENCE

We have conducted experiments aimed at testing the implications of our computational results. Our experimental protocol was as follows. After generating lead sulfide cluster anions, a beam of mass-selected $(PbS)_{32}^-$ cluster anions was gently deposited (soft-landed) onto a highly ordered pyrolytic graphite (HOPG) surface in an ultra-high vacuum environment. There, these clusters lost their charge, diffused across the surface, and aggregated into larger nano-scale objects when they encountered other clusters. The HOPG substrate supporting the deposited and aggregated clusters was then internally transferred from the deposition chamber to adjoining UHV chambers where the sample was interrogated by *in situ* x-ray photoelectron spectrometry (XPS) to perform chemical composition analysis and imaged by *in situ* scanning tunneling microscopy (STM) to measure the approximate lateral and vertical dimensions of the objects on the surface. Figure 5 shows a schematic of our apparatus. The shapes and dimensions of the imaged objects were then compared with those predicted by our calculations. Given the presence of size-defined $(PbS)_{32}$ clusters as the starting point, we were assured that the observed STM images would be the result of

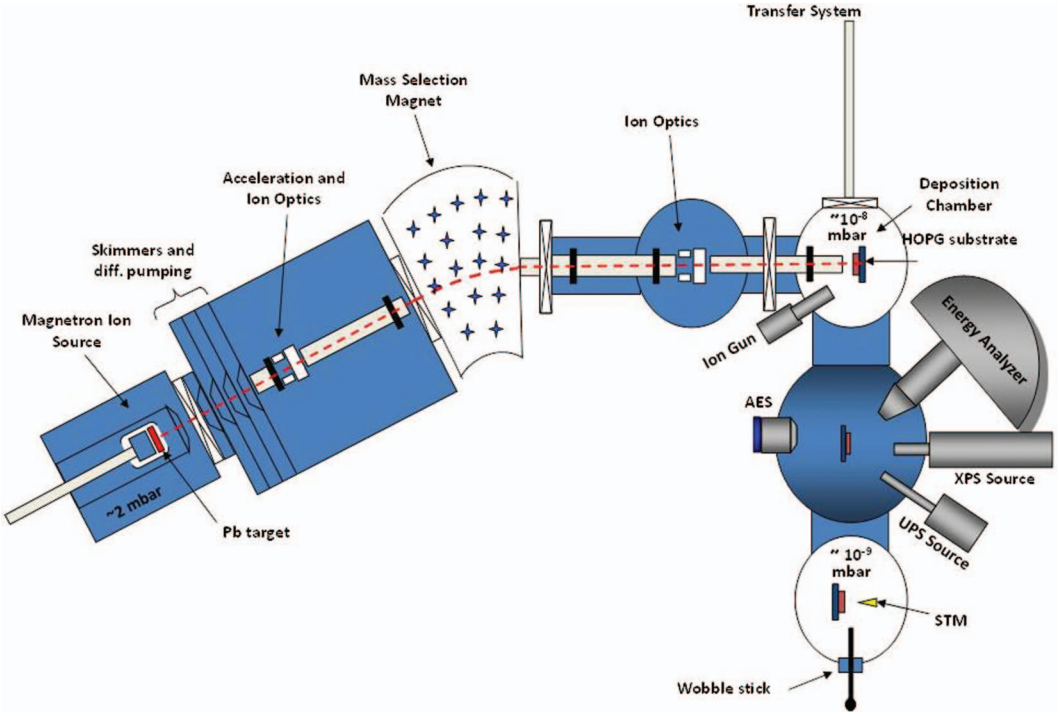

FIG. 5. Schematic of our apparatus, showing the cluster deposition, beam-line, and the surface analytical instrumentation.

two-dimensional nucleation between $(PbS)_{32}$ clusters and/or between nano-blocks composed of multiple $(PbS)_{32}$ units.

Our deposition beam-line has been described in detail in Ref. 14. Briefly, lead sulfide cluster anions were generated by a magnetron source in which a lead target biased at ~300 V was sputtered by argon ions in the presence of argon and H_2S gases. The source was typically operated with a total pressure of ~2 mbars, ~3% of which was H_2S gas. The resulting beam of lead sulfide cluster anions was accelerated to 565 V and passed through a magnetic sector having a resolution of $m/\Delta m = 20$. While the resulting mass-selected beam consisted overwhelmingly of $(PbS)_{32}^-$ cluster anions, some slightly smaller and larger lead sulfide cluster anions, i.e., $(PbS)_{32\pm0.8}$, were also passed by the magnetic sector. The mass scale was calibrated against the mass spectrum of both gold and molybdenum atomic and cluster anions. The mass-selected $(PbS)_{32}^-$ anions were then decelerated to kinetic energies of less than 0.1 eV per atom, and thus soft-landed onto a freshly cleaved, room temperature HOPG surface located in a $\sim10^{-8}$ mbar vacuum environment.

Our surface analytical instrumentation consists of an x-ray photoelectron spectrometer and a scanning tunneling microscope located in adjoining UHV chambers which are also connected to the deposition chamber. Our XPS system is a PHI 5400 instrument equipped with a Mg Kα x-ray source (1253.6 eV). Ejected photoelectrons were measured with a constant pass-energy of 44.75 eV and at a scan rate of 0.125 eV/step. Peak positions were referenced to the C(1*s*) graphite peak (284.5 eV).[15] Our STM system is an Omicron 1 instrument, which operates at room temperature. Hand-cut Pt/Ir tips were used in constant current mode with a gap voltage of 0.7 V and a tunneling current of 0.2 nA. STM image processing was performed using WSxM software.[16] Control experiments were conducted, with and without deposited clusters, to confirm the source of the observed images.

In situ XPS analysis confirmed the chemical composition of the deposited clusters through their measured peaks positions, i.e., the Pb($4f_{7/2}$) transition centered at a binding energy of 137.4 eV and the S($2p_{3/2}$) transition at a binding energy of 160.6 eV.[17] The absence of any spectral intensity in the S(2p) region above 164 eV indicates that there is no sulfur oxidation. This data is shown in Figure 6. The lead to sulfur ratio was also found to be ~1:1, this being based on peak areas and relative sensitivity factors for the pertinent transitions. This composition ratio is consistent with our having deposited mass-selected $(PbS)_{32}$ clusters.

Figure 7 shows a typical STM image of HOPG upon which $(PbS)_{32}$ clusters had been deposited at low coverage. Many of these clusters exhibit square or rectangular-like shapes, consistent with structures formed by the growth of cuboids. Some examples are circled in the figure. This is quite unusual in our experience, where the images of most deposited clusters exhibit round shapes, with no apparent corners.[14] Note that none of the clusters in the STM images have the dimensions of the originally deposited, individual $(PbS)_{32}$ clusters; instead, they are significantly larger. This is because $(PbS)_{32}$ clusters are mobile on HOPG and have aggregated/nucleated into larger objects. We know from our own studies that metal oxide and sulfide clusters in this size regime are extremely mobile on HOPG, and that they aggregate into larger structures. For example, in our studies of mass-selected, soft-landed clusters of both $(WO_3)_{30}$ and $(MoO_3)_{30-60}$ on HOPG,[18,19] AFM images showed aggregated objects and cluster-decorated step edges, a clear indication of cluster mobility. In the present study, STM images of mass-selected, soft-landed $(PbS)_{15}$ clusters also exhibited

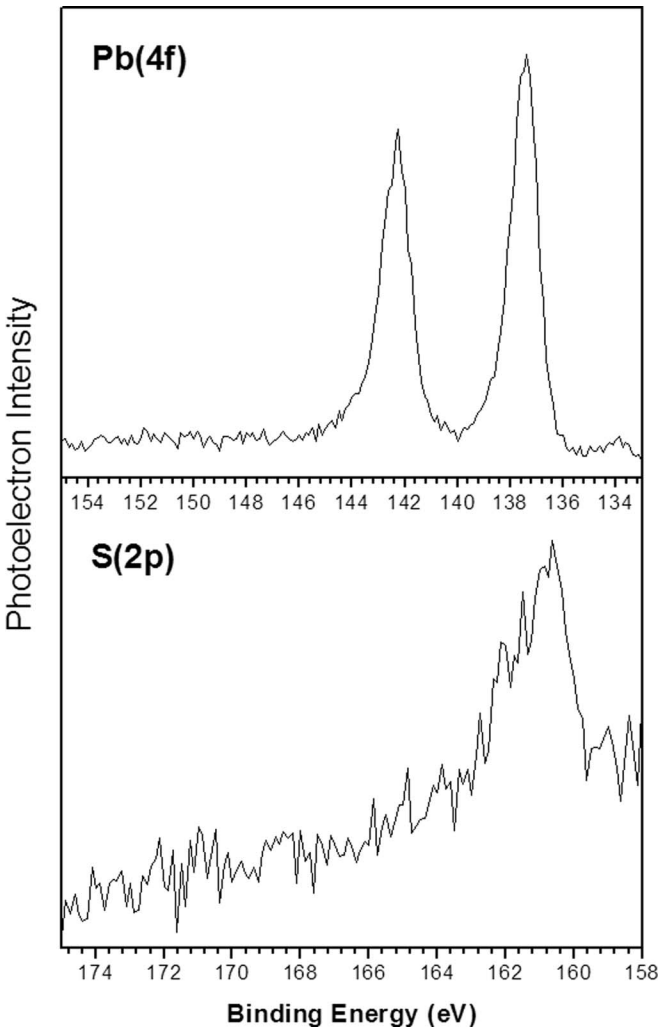

FIG. 6. X-ray photoelectron spectra [Pb(4*f*) and S(2*p*) regions] of lead sulfide aggregates on HOPG.

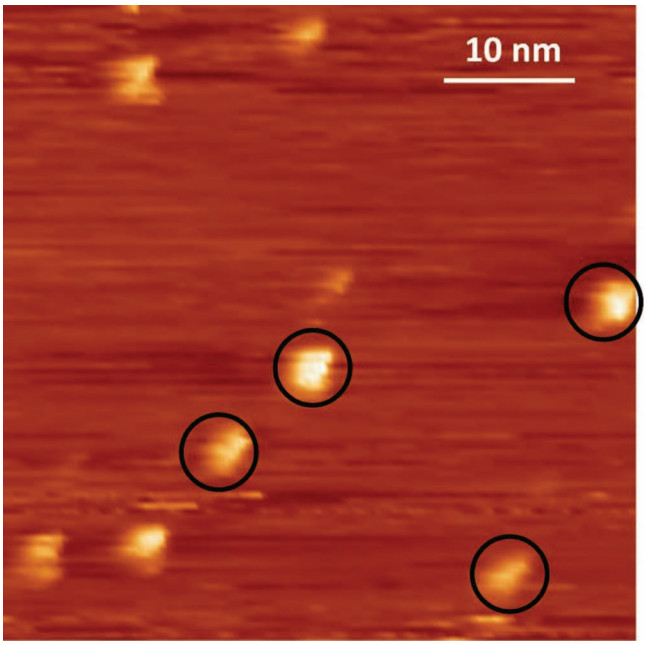

FIG. 7. Scanning tunneling microscope (STM) image of $(PbS)_{32}$ clusters deposited on HOPG.

aggregation and cluster-decorated step edges, i.e., evidence of mobility among $(PbS)_{15}$ clusters. In each of these cases, clusters in this size range appear to have migrated over their HOPG surfaces without a large diffusion energy barrier. It is important to note, however, that square and/or rectangular shapes were not observed among images of aggregated $(PbS)_{15}$ clusters. These angular shapes were unique to images of deposited $(PbS)_{32}$ clusters.

Beyond qualitative assessments of sizes and shapes, STM imaging was also used to determine the approximate lateral and vertical dimensions of clusters on the surface. As described above, our calculations showed that $(PbS)_{32}$ baby crystals can self-assemble to form square or rectangular nano-blocks with theoretically predictable dimensions. We have observed STM images that are consistent with these predictions. Consider, for example, the STM images in Figure 8. There, we have highlighted two representative aggregates. The one labeled, **A**, has measured lateral dimensions, ~2 nm × ~2 nm, while the one labeled, **B**, has measured lateral dimensions, ~4 nm × ~2 nm. The line-scan, presented at the upper left in Figure 8, shows that both aggregates have heights in the range, 0.8–1 nm, consistent with the theoretical prediction of 0.88 nm for structures composed of $(PbS)_{32}$ building blocks. These observations are consistent with our calculations, wherein aggregate **A** is identified as a square $(PbS)_{128}$ nano-block with approximate dimensions, (2 × 2 × 1) nm. This nano-crystal was probably formed due to the dimerization of two $(PbS)_{64}$ clusters, which themselves may have been formed by aggregation of two $(PbS)_{32}$ cuboid clusters. With approximate dimensions, (2 × 4 × 1) nm, aggregate **B** is indentified as a rectangular $(PbS)_{256}$ nano-block. This nano-crystal was probably formed due to the end-on-end dimerization of two $(PbS)_{128}$ clusters. The fact that these two aggregates have the same heights and that they are each approximately 1 nm tall is additional evidence that these are images of theoretically predicted nano-blocks and that their assembly has occurred two-dimensionally. This is not always the case. For example, clusters of mass-selected $(PbS)_{15}$ clusters had grown to much higher heights, e.g., 3–3.5 nm, as they aggregated and sphericalized. The restraint on vertical growth shown by $(PbS)_{32}$-based nano-blocks is due to their crystal-replicating structures as described above.

While face-to-face aggregation between $(PbS)_{32}$ clusters and/or between nano-blocks composed of multiple $(PbS)_{32}$ units was purposeful in our computations, many of the STM images that we recorded suggest that ordered, face-to-face nucleation of nano-blocks also occurred on the actual surface. At first sight, it may seem surprising that the nucleation of nano-crystals would occur in such an organized way. The explanation for this observation may be the crystal growth mechanism known as "oriented aggregation." Unlike classical mechanisms of crystal growth, oriented attachment leads to the coalescence of nucleated nanoparticles into single-crystal-like structures.[20–22]

In addition to trying to understand how ordered nucleation occurred, there is also the issue of why smaller clusters

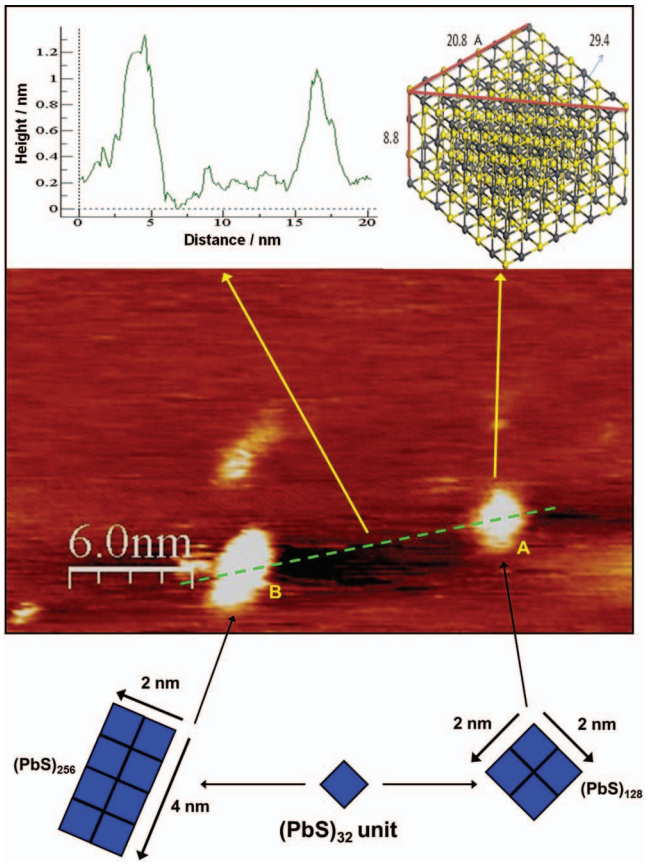

FIG. 8. A STM image showing aggregates resulting from the soft-landing of mass-selected $(PbS)_{32}$ clusters onto a HOPG surface. The cluster at position, **A**, has approximate lateral dimensions of 2 nm × 2 nm, suggesting the side-by-side aggregation of four $(PbS)_{32}$ or two $(PbS)_{64}$ units to form a $(PbS)_{128}$ square nano-block. (A three-dimensional rendering of the structure of $(PbS)_{128}$ is shown at the upper right of this figure.) The cluster at position, **B**, has approximate lateral dimensions of 2 nm ×4 nm, suggesting the side-by-side aggregation of eight $(PbS)_{32}$, four $(PbS)_{64}$, or two $(PbS)_{128}$ units to form a $(PbS)_{256}$ rectangular nano-block. The line-scan across the clusters at positions, **A** and **B**, indicates similar heights in the range of 0.8–1 nm. A plot of height vs. distance along the line-scan is shown in the upper left corner of this figure. Collectively, this data suggests that the nano-blocks at positions, **A** and **B** have dimensions of (2 × 2 × 1) nm and (2 × 4 × 1) nm, respectively.

aggregated into larger ones, such as $(PbS)_{128}$ and $(PbS)_{256}$, and yet continued aggregation seemed to have ceased beyond that size range. As described above, there is ample evidence for mobility and thus aggregation of metal oxides and sulfides in the cluster size regime of $(PbS)_{32}$ and $(PbS)_{64}$. However, our recent work has also found that, at some size, larger metal oxide clusters deposited on HOPG become immobile and stop aggregating.[19] At present, we can only say that we have seen precedents for optimal nucleation size behavior previously.

The realization that clusters can exhibit bulk-like features is not new,[23,24] and $(PbS)_n$ clusters are not the only clusters thought to exhibit bulk-like structures at similar sizes. Calculations on $(MgO)_n$ and $(AgCl)_n$ clusters have also shown them to have bulk-like geometries with sixfold coordination for $n \geq 32$,[25,26] although only our calculations on $(PbS)_n$ clusters have experimental support. The cuboid size, $n = 32$, makes sense when the primitive cell is made up of four diatomic molecules, i.e., when the smallest unit is $n = 4$, a cube of these units requires 8 × 4 or 32 molecules. Interestingly, the bulk crystals of magnesium oxide, silver chloride, and lead sulfide all have rock salt crystal structures. It is tempting to speculate that any bulk material composed of diatomic molecular units and having a rock salt crystal structure might form 64 atom baby crystals, but this is not clear and remains an open question.

SUMMARY

Through calculations, we have demonstrated that $(PbS)_{32}$ is the smallest *cubic* cluster for which its inner $(PbS)_4$ unit enjoys bulk-like coordination, this justifying its designation as a "baby crystal." The calculated dimensions of this special cluster provided a rubric for understanding the pattern of aggregation, i.e., the formation of defined nano-blocks, when they were deposited on a suitable surface. Experiments in which mass-selected $(PbS)_{32}$ clusters were soft-landed onto HOPG and their resulting aggregates imaged by STM provided evidence in support of the computational results. This work was unique in that its theoretical results were supported by experiments, i.e., the STM images were consistent with the theoretically predicted results. This approach provides a pathway for better understanding the mechanisms involved in the formation of solids.

ACKNOWLEDGMENTS

B.K. acknowledges partial support from Shearman Research Initiative Fund. A.K.K. acknowledges support from a McNeese Alumni Association Faculty Development Award. G. G. thanks the DFG (Grant No. GA 389/15-1) for generous support. This material is based upon work supported by the Division of Materials Science and Engineering, Basic Energy Sciences, U.S. Department of Energy, under Grant No. DE-FG02-09ER46558 (K.H.B).

B.K. dedicates this publication to his mentor, Professor E. D. Jemmis, on the occasion of his 60th birthday.

[1] F. Masia, I. Moreels, Z. Hens, W. Langbein, and P. Borri, Phys. Rev. B **82**, 155302 (2010).
[2] S. Wu, H. Zeng, and Z. A. Schelly, Langmuir **21**, 686 (2004).
[3] L. Cademartiri, E. Montanari, G. Calestani, A. Migliori, A. Guagliardi, and G. A. Ozin, J. Am. Chem. Soc. **128**, 10337 (2006).
[4] G. E. Tudury, M. V. Marquezini, L. G. Ferreira, L. C. Barbosa, and C. L. Cesar, Phys. Rev. B **62**, 7357 (2000).
[5] Z. Hens, D. Vanmaekelbergh, E. J. A. J. Stoffels, and H. van Kempen, Phys. Rev. Lett. **88**, 236803 (2002).
[6] P. Koirala, B. Kiran, A. K. Kandalam, C. A. Fancher, H. L. de Clercq, X. Li, and K. H. Bowen, J. Chem. Phys. **135**, 134311 (2011).
[7] M. J. Frisch, G. W. Trucks, H. B. Schlegel *et al.*, GAUSSIAN 03, Revision C.02, Gaussian, Inc., Wallingford, CT, 2004.
[8] J. P. Perdew and Y. Wang, Phys. Rev. B **45**, 13244 (1992).
[9] J. P. Perdew, K. Burke, and Y. Wang, Phys. Rev. B **54**, 16533 (1996).
[10] W. J. Stevens, M. Krauss, H. Basch, and P. G. Jasien, Can. J. Chem. **70**, 612 (1992).
[11] B. Delley, J. Chem. Phys. **113**, 7756 (2000).
[12] J. P. Perdew, Physica B **172**, 1 (1991).
[13] B. Delley, Phys. Rev. B **66**, 155125 (2002).
[14] K. A. Wepasnick, X. Li, T. Mangler, S. Noessner, C. Wolke, M. Grossmann, G. Gantefoer, D. H. Fairbrother, and K. H. Bowen, J. Phys. Chem. C **115**, 12299 (2011).
[15] J. F. Moulder, J. Chastain, P. E. Sobol, and K. D. Bomben, *Handbook of X-ray Photoelectron Spectroscopy: A Reference Book of Standard Spectra for Identification and Interpretation of XPS Data* (Physical Electronics Division, Perkin-Elmer Corp., Eden Prairie, MN, 1992).

[16]I. Horcas, Rev. Sci. Instrum. **78**, 013705 (2007).
[17]A. Osherov, M. Matmor, N. Froumin, N. Ashkenasy, and Y. Golan, J. Phys. Chem. C **115**, 16501 (2011).
[18]X. Li, K. A. Wepasnick, X. Tang, Y. Wang, K. H. Bowen, G. Gantefoer, and D. H. Fairbrother, J. Vac. Sci. Technol. B (submitted).
[19]X. Li, K. A. Wepasnick, X. Tang, Y. Wang, K. H. Bowen, G. Gantefoer, and D. H. Fairbrother (unpublished).
[20]Z. Wang, C. Schliehe, T. Wang, Y. Nagaoka, Y. C. Cao, W. A. Bassett, H. Wu, H. Fan, and H. Weller, J. Am. Chem. Soc. **133**, 14484 (2011).
[21]Q. Zhang, S.-J. Liu, and S.-H. Yu, J. Mater. Chem. **19**, 191 (2009).
[22]M. Niederberger and H. Colfen, Phys. Chem. Chem. Phys. **8**, 3271 (2006).
[23]Q. Sun, B. Rao, P. Jena, D. Stolcic, Y. Kim, G. Gantefor, and A. Castleman, J. Chem. Phys. **121**, 9417 (2004).
[24]C. R. A. Catlow, S. T. Bromley, S. Hamad, M. Mora-Fonz, A. A. Sokol, and S. M. Woodley, Phys. Chem. Chem. Phys. **12**, 786 (2010).
[25]S. Veliah, R. Pandey, Y. S. Li, J. M. Newsam, and B. Vessal, Chem. Phys. Lett. **235**, 53 (1995).
[26]S. Glaus and G. Calzaferri, J. Phys. Chem. B **103**, 5622 (1999).